International Conference on Space Optics—ICSO 2018

Chania, Greece

9–12 October 2018

Edited by Zoran Sodnik, Nikos Karafolas, and Bruno Cugny

Towards qualification longevity of high power Space optics

A. Melninkaitis

G. Batavičiute

C. Heese

M. Šciuka

et al.

International Conference on Space Optics — ICSO 2018, edited by Zoran Sodnik, Nikos Karafolas, Bruno Cugny, Proc. of SPIE Vol. 11180, 1118085 · © 2018 ESA and CNES · CCC code: 0277-786X/18/$18 · doi: 10.1117/12.2536212

Towards qualification longevity of high power space optics

A. Melninkaitis*[a], G. Batavičiūtė[a], C. Heese[b], M. Ščiuka[a], L. Smalakys[a]
[a]UAB Lidaris, Saulėtekio al. 10, 10223 Vilnius, Lithuania;
[b]European Space Agency (ESA/ESTEC), Keplerlaan 1 -
P.O. Box 299 2200 AG Noordwijk ZH, Netherlands

*andrius@lidaris.com;

ABSTRACT

Laser systems dedicated to space missions require durable and well-characterized optics, that could ensure long-term operation under high average output power. If any of optical elements in such system experiences light-induced fatigue, the performance of whole laser system suffers. Thus, any delayed failure of the optical element would also endanger the entire space mission as repairing optic in the orbit is rather complicated. Up to now, the ability to predict optic's longevity required by space programs was difficult and expensive, because of limited experimental data and lack of validated prediction models and methods. In order to address this problem, Lidaris and ESA joined forces for a two years cooperation project ESPRESSO. The overall aim of the project is to carry out research and development work required for essential preparation of reliable longevity qualification procedure to evaluate high power laser optics with intended use in space applications. Main elements of chosen methodology for optics lifetime prediction is reported in this paper. The essence of the proposed method lies in online video detection, failure mode (damage mechanism) separation and subsequent search of appropriate extrapolation models and methods. Main experimental findings confirm the suitability of the suggested approach for prediction of laser-induced damage threshold (LIDT) from a limited set of data to the extrapolated higher number of incident laser pulses.

Keywords: Laser-Induced Damage, Damage Threshold, LIDT, space optic, lifetime, Lidaris, ESA, ESPRESSO

1. INTRODUCTION

It is a well-known fact that optical elements used within high-power laser systems suffer from so-called light-induced fatigue effect, namely – delayed degradation of optical properties due to repetitive exposure to intense laser irradiation. This topic is especially important for long lasting missions that employ UV lasers (for example ESA's Aeolus mission[1]). In order to mitigate risk level associated to degradation of optical components, it is important to select most durable optics with well characterizes performance, so that "safe" laser fluence level and dose could be onset for the entire space mission. As laser-induced damage is often associated with the stochastic process it is necessary to explore a possibility if damage threshold for a particular optical element could be predicted with acceptable uncertainty levels for irradiation dose much larger than the duration of typical damage test. This was the main goal of this study. Thus, we approached prediction of optics lifetime as an interdisciplinary problem involving physical models of failure, statistical methods of data mining, and methods of accelerating lifetime testing.

2. EXPERIMENTAL METHODIC

Experimental set-up

In order to provide meaningful predictions of optics lifetime, it is essential to collect accurate experimental data first. A conventional LIDT test bench was adapted for a long-term measurement at company LIDARIS for this purpose. There were two major concerns to address: long-term stability of laser source and appropriate sensitivity of online damage detection (registration of time to failure events *In situ*). As it has been already demonstrated, LIDT statistics could be affected by nonrepeatable pulses of different temporal shapes (distinct longitudinal modes)[2]. To avoid accidental multi-mode lasing within a long-lasting light burst the injection seeded Nd:YAG diode pumped solid state (DPSS) laser source (NL940-100-SH/TH, EKSPLA) was exclusively designed. It generates single longitudinal mode pulses at 1064 nm, with

100 Hz repetition rate and effective pulse duration ~10 ns (at full width half maximum - FWHM). The light is then frequency doubled and tripled (355 nm) by using nonlinear crystals. Optical beamline of LIDT test bench consists of the three key elements:

1) motorized attenuator – a combination of half-wave plate and polarizer used for a fine fluence adjustment;
2) mechanical shutter used to pick up separate shots from a pulse train with 100 Hz repetition frequency;
3) plano-convex lens used to focus laser irradiation onto the tested sample surface;
4) laser pulse energy is monitored by a calibrated photodiode, registering a fraction of light separated by the beam splitter;
5) spatial beam profile is characterized before and after the measurement by a CCD camera.

The beam diameter for particular testing was set to 209 ± 3 μm at $1/e^2$ level of peak fluence. The sample is placed onto 2 axes (X-Y) motorized translation stage at 45 degrees with respect to laser beam line. Damage events were monitored by two techniques, namely:

1) backscattered light from the irradiated surface by using an online photodiode. Whenever the damage occurs, the signal of backscatter light changes: either it increases in most of the cases or decreases.

2) online differential interference contrast **(**DIC) microscopy – that captures a sequence of images after laser pulses of interest. *In situ* visual inspection is the only way that can provide details of damage evolution dynamics thus it was expected to be a more reliable way for damage event recognition if compared to the self-backscattered light signal. Also, microscopy of the irradiated area provides the principal possibility to distinct nature of different failure modes.

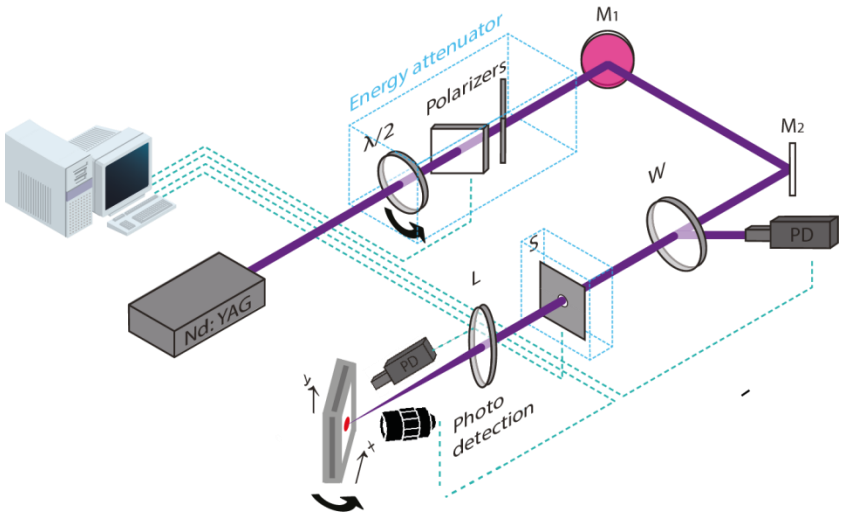

Fig. 1. The schematics of an experimental LIDT test bench. λ/2 is a half-wave plate, M1, M2 are steering mirrors, W - a wedge, L - lens, PD - photodiode, S - mechanical shutter, Photo det. is online DIC microscopy detection unit.

Experimental set of samples

For this experimental study large set of high reflectivity (HR) mirror coatings was prepared. All multilayer dielectric coatings were deposited by using Ion Beam Sputtering (IBS) technique on conventionally polished 25.4 mm in diameter fused silica substrates. The central wavelength of 355 nm was designed to operate at a 45-degree angle of incidence (AOI). Further results for single mirror experiments are described thus representing typical behavior of observed sample set.

Collection of data

In order to predict lifetime, we started from the classical ISO S-on-1 test approach, that is frequently used to benchmark optical materials for laser industry[3]. On the other hand, this kind of test collects data that has a meaning of "time to failure - TTF" events thus we can also interpret them in terms of accelerated lifetime testing. The idea behind S-on-1 is simple: entrance surface of the sample is divided into a virtual matrix of sites to be irradiated with a quite small beam (compared to the whole surface). Each test site is then irradiated with maximum onset laser pulses (for example S = 10 000 in our case) at various fluence level (sometimes also called as stress level). At least 10 sites are irradiated for each fixed fluence. During such irradiation three key variables are recorded:

1) the average and standard deviation of peak fluence at the irradiated site (stress level);

2) microscopy images and the back-scattering signal of each irradiated site, that helps to determine the life status of the irradiated site (after or during irradiation).

3) finally, after DIC image and scattering signal analysis amount (dose) of laser pulses that are required to induce damage (TTF) or reach maximum onset of pulses without damage is recorded;

Calculation of damage probabilities

The data collected as described above can be then interpreted in different ways (either Bayesian approach of damage probability analysis as a function of fluence[4] or Weibull/Survival approach of damage/survival probability as a function of lifetime[5], frequently used with accelerated lifetime testing). Herewith we limit ourselves to damage probability approach. After collection of TTF data at various fluences damage probability is calculated for each class of laser pulses. Damage probability is calculated as a ratio of damaged and total irradiated sites for each onset fluence level (stress) of particular pulse class of interest. It is then plotted as a function of laser fluence (see Fig. 3 for example). By fitting the empirical damage probability curve in the Bayesian way, we get the most probable estimate of threshold fluence (maximum fluence with zero damage probability) that corresponds to laser-induced damage threshold (LIDT). An increased dose of light (number of incident laser pulses) typically ends up in lower LIDTs (fatigue effect). On this point, we have to recall that precise fitting model of damage probability could differ for different samples. In the range of nanosecond laser pulse durations, damage event is usually related to external defects inherent to the manufacturing process (cutting, polishing, cleaning, coating and etc.). As a rule of thumb, such defects are randomly distributed on the sample surface (within first few microns below the surface). By the means of threshold fluence, these defects are often described in form of so called defect ensemble[6–10]. As the distribution of defect thresholds in UV is rather narrow we consider them as identical (all have a constant damage threshold), described by so-called degenerate defect ensemble. Even if this assumption is not absolute it was convenient for the exemplification of the proposed approach. Fit function based on degenerate defect ensemble has two fit parameters: defect density and threshold fluence (LIDT). As it was already mentioned fitting procedure of the damage probability curve is based on the Bayesian approach (Bayesian interference) and is described in[11]. As a result of such data processing, we get a new set of data that will be used for further fatigue analysis: probability density functions PDF(F, N) for each pulse class. Here N – corresponds to N_{th} laser pulse class, and F – to onset fluence respectively. PDFs for higher pulse classes can be significantly constrained or modified by using prior knowledge: Bayes's theorem says that the posterior probability density is the product of the prior probability density and the likelihood function (times a constant). Or in other words, it defines how to update the probabilities of hypotheses when given evidence. For pulse classes $N > 1$ a prior knowledge can be also used:

$$\textbf{Posterior PDF} \sim \textbf{Prior PDF} \times \textbf{Likelihood} \quad (1)$$

The prior distribution is some internal knowledge about the data. For instance, prior can define inequalities such as LIDT for infinite exposure of laser pulses is less than LIDT for single shot irradiation ($F_{inf} \leq F_1$). In the case of LIDT testing, the maximum-likelihood function is constructed based on two key things:

1) the binomial nature of the damage interrogation (either damaged or not after each trial)[12];
2) damage probability model of defect distribution[6–10].

By using Bayesian fitting approach so-called characteristic damage curve (CDC) is obtained, where threshold data point for each pulse class has estimated likelihood distribution. We consider this distribution as a new PDF function when interpreting aging behavior of characteristic damage curve-.

Prediction of optics lifetime: fitting and extrapolation of characteristic damage curve

Each estimated LIDT value in the CDC has a PDF. CDC is then fitted using different mathematical models available in the scientific literature, which are associated with optics lifetime degradation (fatigue). It is based on the Bayesian approach. First of all, we compose likelihood function out of experimentally measured PDF's and candidate models simulating experimental characteristic damage curves. The general form of likelihood could be described as follows:

$$L = \prod_{i=1}^{S} PDF_i\left(F_{th}(N_i)|\theta(N_i)\right) \quad (2)$$

Here, S – amount of pulse classes of interest, PDF_i – estimated likelihood distribution of threshold parameter for i_{th} pulse class as described in[4], $F_{th}(N)$ – chosen aging model of characteristic damage curve, N_i – number of incident laser pulses for particular class, $\theta(N_i)$- set of experimental data: empirical probability and chosen model of defects to fit damage probability. To find best fit (maximum L) for each $F_{th}(N)$ function parameters should be varied. The LIDT values estimated from damage probability curves are plotted versus the incident number of laser pulses - CDC. In order to predict optics lifetime CDC should be extrapolated by using best estimates of fitted model parameters. However, best fit says nothing about the measurement uncertainty. In order to estimate the uncertainty of extrapolation Markov Chain Monte Carlo Method (MCMC) is used[13]. MCMC procedure provides a sampled distribution of extrapolated model parameters. Two statistical techniques were used to interpret empirical extrapolated distribution, namely assumed distribution fitting and Kernel Density Estimation (KDE)[14,15]. Distributions of the best estimates are determined by MCMC procedure. However, this time, LIDT is not (is not necessary to be) the parameter of the fit model. In order to extract LIDT distribution a large number of random extrapolation curves are generated using MCMC samples. Then obtained sample distribution is used to calculate Cumulative Distribution Function (CDF and Percent Point Function (PPD)). Percent Point function is an inverse CDF. In this way, limited experimental data could be extracted to the high number of laser pulses. This method was validated experimentally.

3. SEARCH FOR AN APRROPRIATE FATIGUE MODEL

Usually, LIDT CHD curve $F_{th}(N)$ or fatigue function (in some context could be also called as Life-Stress relationship or link function) is unknown prior to the measurement. Variety of mathematical models have been reported in the scientific literature. In our work measured CDC is fitted to eight mathematical models summarized in Table 1. However, different statistical models predict events with different adequacy.

Table 1. Mathematical candidate models simulating experimental characteristic damage curves.

Mathematical model	
Power Law (Jee et al) [16]	$F_{th}(N) = F_1 N^{S-1}$
Power Law (Neuenschawander et al) [16,17]	$F_{th}(N) = F_{inf} + F_1 N^{S-1}$
Logarithmic [18–21]	$F_{th}(N) = b - a\ln(N)$
Logarithmic ISO[3]	$F_{th}(N) = F_{inf} + \frac{F_1 - F_{inf}}{1 + \left(\frac{1}{\Delta}\right)\lg(N)}$
Exponential (Ashkenasi et al) [22–27]	$F_{th}(N) = F_{inf} + \left(F_1 - F_{inf}\right)e^{-k(N-1)}$
Exponential (Arrenberg et al I) [28]	$F_{th}(N) = F_{inf} + ae^{(-bN)}$
Exponential (Arrenberg et al II) [28]	$F_{th}(N) = F_{inf} + ae^{(-bN)} + ce^{(-dN)}$
Mixed (Allenspacher et al) [29]	$F_{th}(N) = F_1 e^{(-N/c_1)} + F_2 N^{(-c_2)}$

Here, N is amount of incident laser pulses, F_{inf} – is the constant threshold for $N = \infty$, $F_1 + F_{inf}$ is single pulse damage threshold, a, b, c, c_1, c_2, d, Δ, d, S – various model parameters. To find the most appropriate model it is desirable necessary to have as many candidate functions as possible. Models that are either too flexible or not able to describe the main trends in data are judged by using Goodness of the Fit (GoF) concept[30,31]. GoF is evaluated using two steps: first we obtain GoF indices and later compare GoF statistics[31]. GoF indices summarize the discrepancy between the observed data and the values expected under a statistical model. GoF statistics are GoF indices with known sampling distributions, usually obtained using asymptotic methods which are used in statistical hypothesis testing. - It is important to note, that GoF does not imply the validity of best performing model, but rather roughly selects the best candidate out of tested models. There are various modifications of GoF tests. The logic behind these tests is similar in all cases, however, they differ in how the test statistics and critical values are calculated. In this study, we compare GoF by the means of Akaike Information Criteria (AIC)[32]. As soon as global maxima is found we get L - the maximum value of the likelihood function for interrogated model; let k be the number of free parameters in $F_{th}(N)$ model. The AIC value of the model is obtained as follows:

$$\mathrm{AIC} = 2 \cdot k - 2\ln(L) \tag{3}$$

Given a set of candidate models for the data, the preferred model is the one with the minimum AIC value. AIC rewards goodness of fit (as assessed by the likelihood function), but it also includes a penalty for model flexibility for a larger amount of model parameters. The penalty discourages overfitting (increasing the number of parameters in the model almost always improves the goodness of the fit). Accordingly, AIC is evaluated for each fatigue model used to fit experimental results. There are two ways to compare models by Akaike Information criterion.

1) The delta AIC - the difference between AIC of the model of interest and AIC of the model, with minimum AIC value. Suitability of the model is evaluated by delta AIC absolute values, following the rule of thumbs.
2) The Akaike weights are obtained by the ratios of a candidate model's delta AIC relative to the sum of the delta AICs for all candidate models. It defines the probability that the candidate model is the best among the set of candidate models. For example, if a candidate model has an Akaike weight of 0.60, this means that given the data, the candidate model has a 60% probability of being the best one.

Even if we find the most probable model it is only best form the family of investigated candidates, however extrapolation still needs to be validated against real life data of observations outside the region existing data.

4. RESULTS AND DISCUSSION

Failure mode separation

Two types of permanent changes (damage mechanisms/modes) have been identified in recorded images for the tested sample (fig. 2), namely:

1. Early defect driven damage. The damage consisting of randomly localized dark dots, typically appear in random places when irradiated with the large beam. There is no direct correlation between damage morphology and spatial distribution of the irradiated beam;
2. Late non-catastrophic color change – apparent by Nomarski microscopy as smooth dark area nicely replicating beam intensity pattern on the sample surface.

Also, as it is shown in Fig. 2 (bottom row), different damage modes can co-exist together, thus also screening each other. In this particular case, the test site is considered as damaged after 1 pulse when estimating "defect driven" damages and is only damaged after 3000 pulses when estimating "color change" mode. Interestingly, for the investigated test sample, defect driven damages always appeared within the first 1-10 laser pulses while most of the color change type of damages started only after 3000 laser pulses or more at the same laser fluence level. The "color change" was the only type of damage, which occurred for the higher number of laser pulses (100k, 1M, and 10M). The S(10.000)-on-1 test results were interpreted separately for each failure mode. To investigate trends in laser-induced damage threshold both failure modes should be identified and interpreted in isolation from each other.

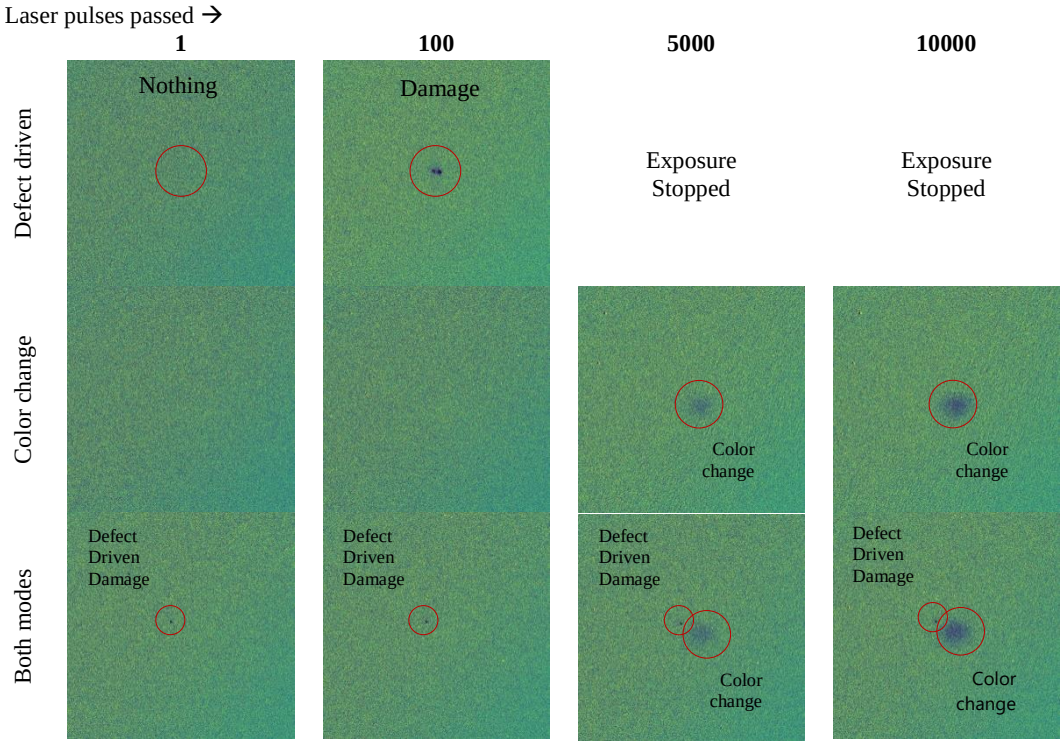

Fig. 2. Evolution of the typical laser-induced damage morphologies obtained by Nomarski (DIC, 10x) microscopy for the fluence slightly below single shot damage threshold.

S(10.000)-on-1 LIDT results

After visual morphology analysis damage statistics were separated into two groups and probability curves were calculated in isolation (for each failure mode) for every particular laser pulse class. Fluence dependencies of separated failure mode probabilities are shown in (Fig. 3). The statistics of catastrophic defect driven damage is rather random and is almost "frozen" after 10 laser pulses. Damage associated with color change features quite deterministic damage behavior that is "moving" toward left side when the amount of irradiated pulses is increasing. This behavior suggests a non-saturated incubation effect.

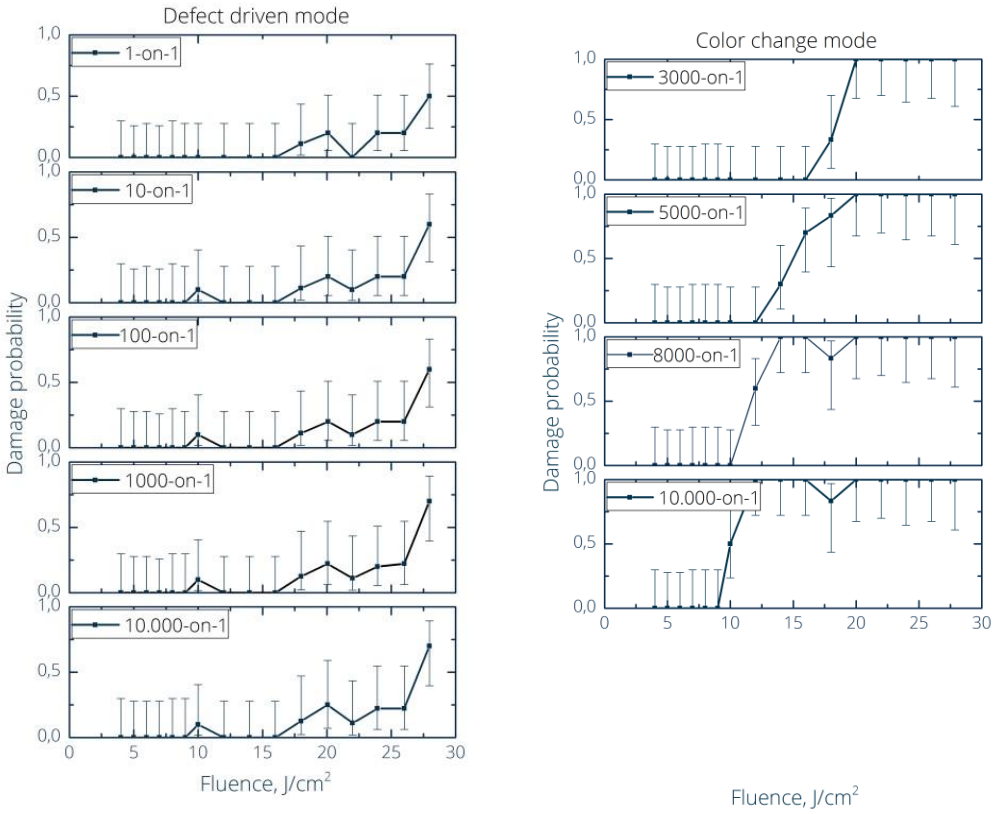

Fig. 3. Damage probabilities at various pulse classes calculated by using different LID criteria: defect driven damage – on the left, color change – on the right.

By fitting damage probability curves with degenerate model characteristic damage curves calculated for pulse classes that contain meaningful data. For such fitting maximum likelihood approach is used, that has both S(10.000)-on-1 LIDT test for each damage mode (or detection method) are shown in the Fig. 4. They are visualized as lines with scatter either square or dot. Calculated LIDT values are summarized in Table 2.

Table 2. Calculated LIDT values from S(10.000)-on-1 LIDT test using 2 different LID criteria.

Pulse class	LIDT, J/cm² (calculated from measurement)										
	Catastrophic Defect Driven Mode						Color Change Mode				
	Lower confidence band		LIDT		Upper Confidence band		Lower confidence band		LIDT		Upper Confidence band
1	12.00	≤	15.99	≤	17.86		-	≤	-	≤	-
10	6.17	≤	8.97	≤	9.96		-	≤	-	≤	-
100	6.18	≤	8.97	≤	9.92		-	≤	-	≤	-
1000	6.09	≤	8.97	≤	9.92		-	≤	-	≤	-
3000	6.09	≤	8.97	≤	9.92		14.30	≤	15.99	≤	17.43
5000	6.09	≤	8.97	≤	9.92		10.07	≤	12.00	≤	13.24
8000	6.09	≤	8.97	≤	9.92		8.05	≤	8.97	≤	10.35
10000	6.35	≤	8.97	≤	9.97		6.87	≤	8	≤	9.01

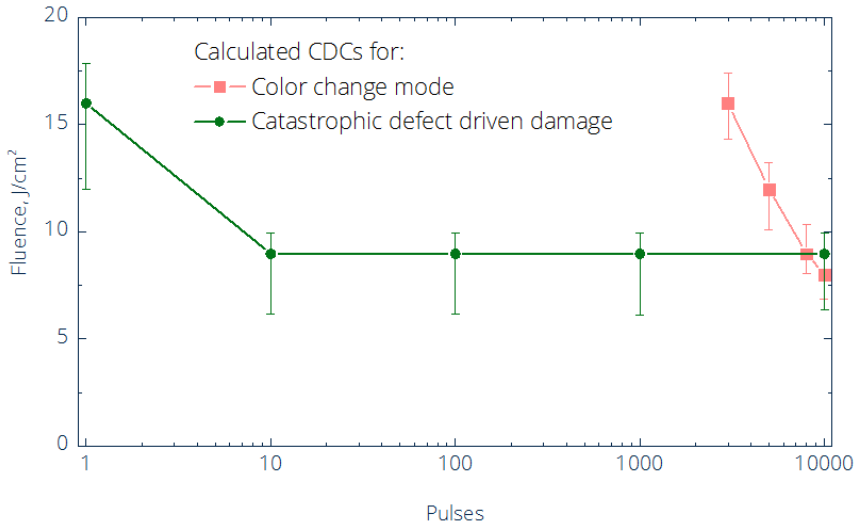

Fig. 4. Characteristic damage curves calculated LIDT values from S(10.000)-on-1 LIDT test using 2 different LID criteria.

Results show that defect driven damage mode (green) features an abrupt decrease in LIDT within a first few laser pulses and after approaches almost asymptotic constant level. This was a typical observation defect limited characteristic damage curve. On the contrary "Color change" type of mode starts quite late at around 3000 laser pulses. The LIDTs at 10k laser pulses corresponding to both failure modes are quite similar, but the trends and shapes of the CDC are very different. Color changing mode goes down without saturation thus suggesting a further monotonic decay.

5. VALIDATION OF FITTED MODELS

In Table 3 we summarized GoF of fitted model candidates. In some cases, we were not able to fit a particular model, thus meaning that the model was not relevant. In some cases, we were unable to select only one best fitting model. In the case of defect driven mode, we found that pretty much each model, which features asymptotic behavior, could be used to fit data. We chose an exponential model presented by Ashkenasi et al[22–27] for further analysis. Yet any other suggested model provided similar results. In the case of color change mode, we found two best candidates namely logarithmic[18–21] and power law[16,17]. We have examined both models. The logarithmic model predicted rapid LIDT decrease within the next additional thousands of laser pulses. Based on validation data this model was later rejected. Thus, the power law model as suggested by Jee et al[16] was used for further analysis.

Table 3. Mathematical models used to fit S(10.000)-on-1 LIDT data.

Mathematical model:	**GoF based analysis of Characteristic damage curve**	
Failure Mode:	Defect driven	Color change
Power Law (Jee et al) [16]	FAILED	BEST
Power Law (Neuenschawander et al) [16,17]	BEST	POSSIBLE
Logarithmic [18–21]	FAILED	BEST
Logarithmic ISO[3]	BEST	NOT SUITED
Exponential (Ashkenasi et al) [22–27]	BEST	NOT SUITED
Exponential (Arrenberg et al I) [28]	BEST	NOT SUITED
Exponential (Arrenberg et al II) [28]	POSSIBLE	NOT SUITED
Mixed (Allenspacher et al) [29]	POSSIBLE	POSSIBLE

Extrapolated CDCs from 10k laser pulses to 10M laser pulses are shown in the Fig. 5. Scatter and line represent calculated LIDT from S(10.000)-on-1 LIDT test. The filled area shows extrapolation by selected models. Numbers 0.01 and 0.99

next to the fit represent damage probabilities at particular fluencies and laser pulses. In order to validate extrapolation, multiple points were tested below measured 10k-on-1 damage threshold with the significantly higher dose of incident laser pulses (namely 1M and 10M). All damages from online images recorded with DIC based damage detection unit were identified as color change only. The lowest observed damages for each pulse class are plotted as the black scatters points in the graph. Since online images were taken for fixed time intervals the data are interval-censored. These intervals are represented as horizontal error bars for each validation point.

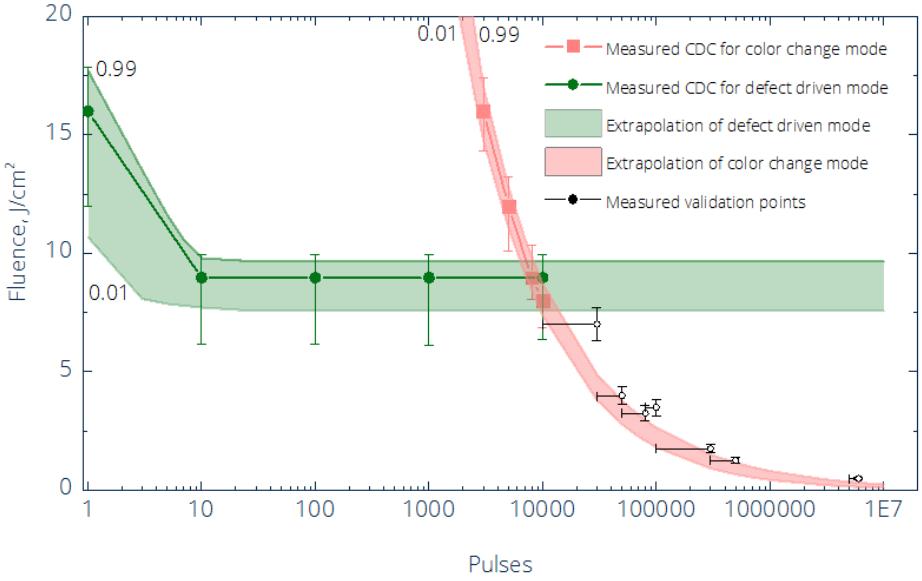

Fig. 5. Extrapolated characteristic damage curves and model validation points measured at high number of incident laser pulses.

The presented results visualize very different behavior for distinct failure modes. It shows, that defect driven damage mode is stochastic and its extrapolation highly overestimates LIDT as it is screening “color changing” mode. It corresponds to child mortality mechanism describing the beginning of the widely known “Bathtub” curve. The “Color change” damage mode is quite deterministic and has a clear shape, thus could be used to predict real LIDT behavior at the high number of incident laser pulses with good confidence. Both the shape of the model and predicted absolute values matches the measured data in the range of MCMC predicted uncertainty. These results suggest that developed measurement and extrapolation methodology combined with DIC based analysis is capable to predict LIDT from a limited set of data to the higher number of incident laser pulses.

6. CONCLUDING REMARKS

For the first time, two types of laser-induced degradation mechanisms were identified and analyzed in highly reflecting dielectric coatings when irradiating with repetitive nanosecond UV laser pulses. Defect driven - fatigue and laser-induced gradual color change were identified as signs of distinct mechanisms of degradation. Both mechanisms appear simultaneously and thus screen each other making any prediction not possible. Thanks to proposed online video detection scheme we were able to distinguish statistics corresponding to each failure mode and analyze both data groups in isolation from each other. By doing so we were able to identify best fitting candidate models presumably able to predict damage behavior for larger irradiation dose. Power law model was identified as a best fitting model to describe threshold behavior of color change, while defect driven damage seems to saturate at certain fluence level after first 10 pulses. Accordingly, more functions could be used to describe saturated behavior. Distinct mechanisms indicated very different trends in LIDT with increasing dose of laser pulses. Validations experiments suggest that proposed approach could be used for induced aging prognosis in laser optics with high confidence.

ACKNOWLEDGEMENT

This work was performed within the framework of joint Lidaris – ESA project "ESsential PREparation Steps for Qualification Longevity of Space Optics" (ESPRESSO, PECTS call, Contract Nr. 4000115898). The view expressed herein can in no way be taken to reflect the official opinion of the European Space Agency.

REFERENCES

[1] ESA., "Introducing Aeolus - ESA's wind mission," 2018, <https://www.esa.int/Our_Activities/Observing_the_Earth/Aeolus> (22 August 2018).
[2] Batavičiute, G., Pupka, E., Pyragaite, V., Smalakys, L.., Melninkaitis, A., "Effect of longitudinal laser mode beating in damage probability measurements," Proc. SPIE - Int. Soc. Opt. Eng. **8885** (2013).
[3] ISO., "ISO Standard No. 21254-1 :2011 ; ISO Standard No. 21254-2 :2011" (2011).
[4] Batavičiute, G., Grigas, P., Smalakys, L.., Melninkaitis, A., "Revision of laser-induced damage threshold evaluation from damage probability data," Rev. Sci. Instrum. **84**(4) (2013).
[5] Nelson, W., Accelerated testing : statistical models, test plans and data analyses, Wiley-Interscience (2004).
[6] Porteus, J. O.., Seitel, S. C., "Absolute onset of optical surface damage using distributed defect ensembles.," Appl. Opt. **23**(21), 3796 (1984).
[7] O'Connell, R. M., "Onset threshold analysis of defect-driven surface and bulk laser damage.," Appl. Opt. **31**(21), 4143–4153 (1992).
[8] Krol, H., Gallais, L., Grèzes-Besset, C., Natoli, J. Y.., Commandré, M., "Investigation of nanoprecursors threshold distribution in laser-damage testing," Opt. Commun. **256**(1–3), 184–189 (2005).
[9] Natoli, J.-Y., Gallais, L., Akhouayri, H.., Amra, C., "Laser-induced damage of materials in bulk, thin-film, and liquid forms.," Appl. Opt. **41**(16), 3156–3166 (2002).
[10] Melninkaitis, A., Bataviciute, G.., Sirutkaitis, V., "Numerical analysis of laser-induced damage threshold search algorithms and their uncertainty," Proc. SPIE **7504**, 75041D–75041D–12 (2009).
[11] Bulgakova, N. M., Bulgakov, A. V.., Babich, L. P., "Energy balance of pulsed laser ablation: thermal model revised," Appl. Phys. a-Materials Sci. Process. **79**(4–6), 1323–1326 (2004).
[12] Hildenbrand, A., Wagner, F. R., Akhouayri, H., Natoli, J.-Y.., Commandré, M., "Accurate metrology for laser damage measurements in nonlinear crystals," Opt. Eng. **47**(8), 83603 (2008).
[13] van Ravenzwaaij, D., Cassey, P.., Brown, S. D., "A simple introduction to Markov Chain Monte–Carlo sampling," Psychon. Bull. Rev. **25**(1), 143–154, Springer US (2018).
[14] Rosenblatt, M., "Remarks on Some Nonparametric Estimates of a Density Function," Ann. Math. Stat. **27**(3), 832–837, Institute of Mathematical Statistics (1956).
[15] Parzen, E., "On Estimation of a Probability Density Function and Mode," Ann. Math. Stat. **33**(3), 1065–1076, Institute of Mathematical Statistics (1962).
[16] Neuenschwander, B., Jaeggi, B., Schmid, M., Dommann, A., Neels, A., Bandi, T.., Hennig, G., "Factors controlling the incubation in the application of ps laser pulses on copper and iron surfaces," Proc. SPIE **8607**, X. Xu, G. Hennig, Y. Nakata, and S. W. Roth, Eds., 86070D, International Society for Optics and Photonics (2013).
[17] Di Niso, F., Gaudiuso, C., Sibillano, T., Mezzapesa, F. P., Ancona, A.., Lugarà, P. M., "Role of heat accumulation on the incubation effect in multi-shot laser ablation of stainless steel at high repetition rates," Opt. Express **22**(10), 12200, Optical Society of America (2014).
[18] Gallais, L., Natoli, J.., Amra, C., "Statistical study of single and multiple pulse laser-induced damage in glasses.," Opt. Express **10**(25), 1465–1474 (2002).
[19] Natoli, J. Y., Bertussi, B.., Commandré, M., "Effect of multiple laser irradiations on silica at 1064 and 355 nm.," Opt. Lett. **30**(11), 1315–1317 (2005).
[20] Ling, X., "Nanosecond multi-pulse damage investigation of optical coatings in atmosphere and vacuum environments," Appl. Surf. Sci. **257**(13), 5601–5604, Elsevier B.V. (2011).
[21] Herringer, J., Riede, W., Ciapponi, A., Allenspacher, P.., Arenberg, J., "An empirical investigation of the laser survivability curve: III," 4 December 2012, 85301N, International Society for Optics and Photonics.
[22] Ashkenasi, D., Lorenz, M., Stoian, R.., Rosenfeld, a., "Surface damage threshold and structuring of dielectrics using femtosecond laser pulses: the role of incubation," Appl. Surf. Sci. **150**(1), 101–106 (1999).

[23] Rosenfeld, a., Lorenz, M., Stoian, R.., Ashkenasi, D., "Ultrashort-laser-pulse damage threshold of transparent materials and the role of incubation," Appl. Phys. A Mater. Sci. Process. **69**(7), 373–376 (1999).
[24] Wang, X. C., Lim, G. C., Zheng, H. Y., Ng, F. L., Liu, W.., Chua, S. J., "Femtosecond pulse laser ablation of sapphire in ambient air," Appl. Surf. Sci. **228**(1–4), 221–226 (2004).
[25] Liang, F., Vallée, R., Gingras, D.., Chin, S. L., "Role of ablation and incubation processes on surface nanograting formation," Opt. Mater. Express **1**(7), 1244, Optical Society of America (2011).
[26] Ashkenasi, D., Rosenfeld, A.., Stoian, R., "Laser-induced incubation in transparent materials and possible consequences for surface and bulk microstructuring with ultrashort pulses," 5 April 2002, 90, International Society for Optics and Photonics.
[27] Kern, C., Zürch, M., Petschulat, J., Pertsch, T., Kley, B., Käsebier, T., Hübner, U.., Spielmann, C., "Comparison of femtosecond laser-induced damage on unstructured vs. nano-structured Au-targets," Appl. Phys. A **104**(1), 15–21, Springer-Verlag (2011).
[28] Arenberg, J., Riede, W., Ciapponi, A., Allenspacher, P.., Herringer, J., "An empirical investigation of the laser survivability curve," 13 October 2010, 78421B, International Society for Optics and Photonics.
[29] Allenspacher, P., Riede, W., Wernham, D., Capanni, A.., Era, F., "Vacuum laser damage test bench," 5 October 2005, 599128, International Society for Optics and Photonics.
[30] Bagdonavicius, V.., Nikulin, M., Accelerated Life Models, Chapman and Hall/CRC (2001).
[31] Maydeu-Olivares, A.., García-Forero, C., "Goodness-of-Fit Testing," [International Encyclopedia of Education], Elsevier, 190–196 (2010).
[32] Akaike, H., "Information Theory and an Extension of the Maximum Likelihood Principle," Springer, New York, NY, 199–213 (1998).